THE JOURNAL OF PHYSICAL CHEMISTRY Letters

Letter

pubs.acs.org/JPCL

Vibrational Predissociation of the HCl−$(H_2O)_3$ Tetramer

Kristen Zuraski, Daniel Kwasniewski, Amit K. Samanta, and Hanna Reisler*

Department of Chemistry, University of Southern California, Los Angeles, California 90089-0482, United States

Supporting Information

ABSTRACT: The vibrational predissociation of the HCl−$(H_2O)_3$ tetramer, the largest HCl−$(H_2O)_n$ cluster for which HCl is not predicted to be ionized, is reported. This work focuses on the predissociation pathway giving rise to H_2O + HCl−$(H_2O)_2$ following IR laser excitation of the H-bonded OH stretch fundamental. H_2O fragments are monitored state selectively by 2 + 1 resonance-enhanced multiphoton ionization (REMPI) combined with time-of-flight mass spectrometry (TOF-MS). Velocity map images of H_2O in selected rotational levels are used to determine translational energy distributions from which the internal energy distributions in the pair-correlated cofragments are derived. From the maximum translational energy release, the bond dissociation energy, $D_0 = 2400 \pm 100$ cm^{-1}, is determined for the investigated channel. The energy distributions in the fragments are broad, encompassing the entire range of allowed states. The importance of cooperative (nonpairwise) interactions is discussed.

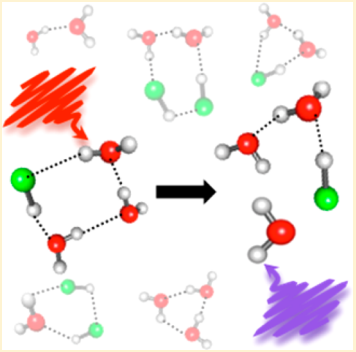

The interaction of HCl with water is of fundamental interest as a prototype of acid solvation. The ability of polar solvents to stabilize ions in solution is well-known; however, the energetics, dynamics, and mechanisms of this process have not been completely elucidated yet at the molecular level. Beyond fundamental interest, the solvation of HCl on polar stratospheric clouds creates an activated form of chlorine in the upper atmosphere that is expected to play an important role in the ozone depletion cycle.[1−3] It is no wonder, therefore, that studies of HCl in water in different environments and temperatures continue to attract much attention. Small HCl/H_2O clusters afford a way of adding water molecules one at a time until acid ionization is reached, but experimental studies have been challenging.

Review articles summarizing previous studies of H_2O and/or HCl clusters have recently been published.[4−6] Results of theoretical studies demonstrate that as the number of water molecules in a cluster with a single HCl molecule increases, the hydrogen bond (H-bond) lengths are reduced and the red shifting of the HCl and OH stretch frequencies increases.[7−11] These trends suggest an increase in H-bonding strength. For larger HCl−$(H_2O)_n$ clusters, a sequential proton transfer finally generates $Cl^-(H_2O)_{n-1}H_3O^+$, a stable, solvent-separated ion pair.[11−15] According to theoretical studies, whether ionization occurs at n = 4 or 5 depends on temperature and experimental conditions.[15−18]

Few experimental studies are reported on the vibrational spectroscopy of small HCl−$(H_2O)_n$ clusters in a molecular beam due to difficulties encountered in assigning their infrared (IR) spectra.[19−24] Specifically, when a mixture of HCl and H_2O is expanded, $(HCl)_m$−$(H_2O)_n$ clusters with several m and n combinations are formed, and probing selected clusters depends on the ability to assign their spectra. The spectra contain broad peaks from larger clusters overlaid with sharper peaks from smaller clusters with m = 0−4 and n = 1−4.[19,25] The theoretical studies of Mancini and Bowman identified spectroscopic features in the regions of the OH and HCl stretch vibrations, but within the accuracy of the theoretical treatment, it was difficult to assign conclusively features belonging to specific clusters.[26] Fortunately, Zischang et al.[20] have recently reported experimental assignments of the H-bonded OH stretch fundamentals at 3100−3700 cm^{-1}, which have made the vibrational predissociation (VP) study reported here feasible.

Through the study of neutral cluster systems such as HCl−$(H_2O)_n$ (n = 1−3), it is possible to observe trends and changes in the H-bond dissociation energy (D_0) and the effect of cooperativity. The work presented here describes the first results on the VP of the HCl−$(H_2O)_3$ tetramer, the largest cluster for which ionization of HCl is not expected. Theoretical studies conclude that the optimized geometry HCl−$(H_2O)_3$ is cyclic,[7−9,12,20,26,27] as shown in Scheme 1, and the strength of the H-bonds is expected to decrease in the order α, β, γ, δ.

Following excitation of the H-bonded OH stretch fundamental, only two dissociation pathways are possible (Scheme 2): Pathways 1 and 2 yield HCl−$(H_2O)_2$ + H_2O and HCl + $(H_2O)_3$,

Scheme 1. Structure of HCl−$(H_2O)_3$ Tetramer

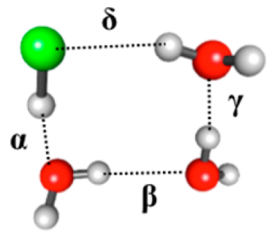

Received: August 16, 2016
Accepted: October 10, 2016
Published: October 10, 2016

DOI: 10.1021/acs.jpclett.6b01848
J. Phys. Chem. Lett. 2016, 7, 4243−4247

Scheme 2. Energetically Allowed Pathways for Dissociation of $HCl-(H_2O)_3$

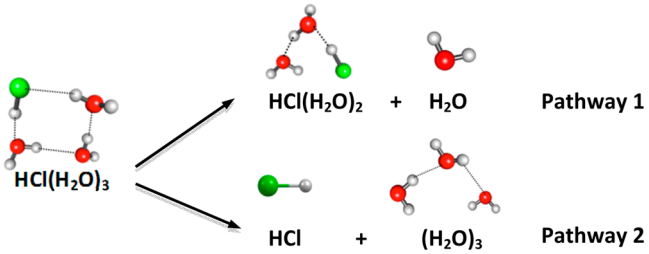

respectively. By selectively monitoring H_2O fragments after VP, Pathway 1 was isolated for the present study, and the bond dissociation energy and distribution of energy in the products were determined.

Experimental results most relevant to the present study include: (1) the VP dynamics of the $HCl-H_2O$ dimer,[28] and (2) the observation of a large shift in the dipole moments of $DCl-(H_2O)_n$ between $n = 5$ and 6.[29] This latest work indicates a change in the structure that is characteristic of acid solvation, but the observations are open to other interpretations as well. Other spectroscopic investigations[21] address infrared signatures of ionization with $n = 4$ water molecules.

Characterization of the fundamental OH stretch region was crucial for our studies as it allowed for tagging $HCl-(H_2O)_3$ while at the same time inducing dissociation. Zischang et al.[20] have shown that based on experimental observations and ab initio calculations, several transitions are likely associated with the H-bonded OH stretch fundamentals of $HCl-(H_2O)_3$ in helium nanodroplets: 3560.1, 3546.8, 3476.2, and 3438.5 cm^{-1}. We have obtained IR action spectra in a supersonic molecular beam (helium carrier gas) in the range of 3520−3655 cm^{-1} by monitoring state-selected H_2O fragments ($J''_{Ka,Kc} = 2_{2,1}$, $3_{2,1}$, $5_{0,5}/5_{1,5}$, $7_{1,6}$) by 2 + 1 REMPI. Our results show several peaks whose intensities vary with the HCl/H_2O ratio in the expansion. On the basis of our measured pressure and concentration dependencies of the action spectra and comparisons with previous spectroscopic work, we assign the intense broad peak observed at 3530−3555 cm^{-1} to excitation of the H-bonded OH stretch fundamental of $HCl-(H_2O)_3$. This is most likely analogous to the 3546.8 cm^{-1} peak observed in the helium droplet study [see the Supporting Information for a detailed discussion of the justification of our assignment and comparisons of our action spectra with previous results]. VP was induced by pulsed laser excitation in this band at 3550 cm^{-1}, which has minimum overlap with other HCl/H_2O mixed clusters and pure water clusters. Figure 1 shows a representative spectrum obtained by detecting $H_2O(J''_{Ka,Kc} = 3_{2,1})$ in the region of 3520−3560 cm^{-1}. Similar action spectra were observed by detecting $HCl(J'')$ states, albeit with higher background from larger clusters and lower signal-to-noise ratio.

A photofragment yield spectrum was obtained by exciting $HCl-(H_2O)_3$ at 3550 cm^{-1} and scanning the UV laser frequency in the region of the $\tilde{C}^1B_1(000) \leftarrow \tilde{X}^1A_1(000)$ H_2O transition. Figure 2 displays the 2 + 1 REMPI spectrum of H_2O fragments and the background spectrum of water monomers. Fast predissociation in the $\tilde{C}$ state and spectral congestion limit the state-selective detection of H_2O.[28] The highest isolated rotational state detected in our study was $J''_{Ka,Kc} = 7_{1,6}$ (704 cm^{-1}), which sets an upper limit to D_0 at approximately 2850 cm^{-1} for Pathway 1. A more accurate value is obtained by Velocity Map Imaging (VMI). By careful selection of the UV wavelength,[30,31]

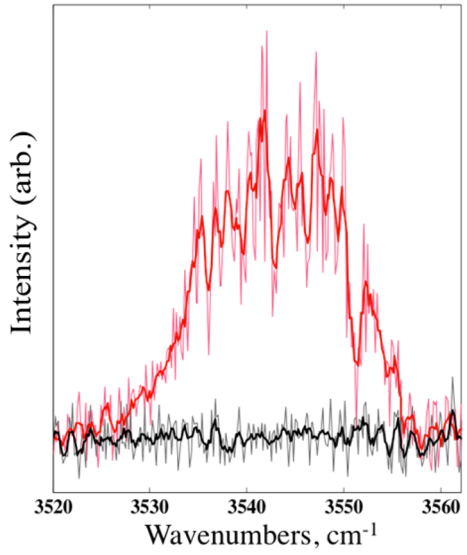

Figure 1. IR action spectrum (red) obtained by monitoring the H_2O photofragment in $J''_{Ka,Kc} = 3_{2,1}$. The black line shows the background from H_2O monomers. The raw data are shown in lighter color, and bold lines show the data with three-point smoothing.

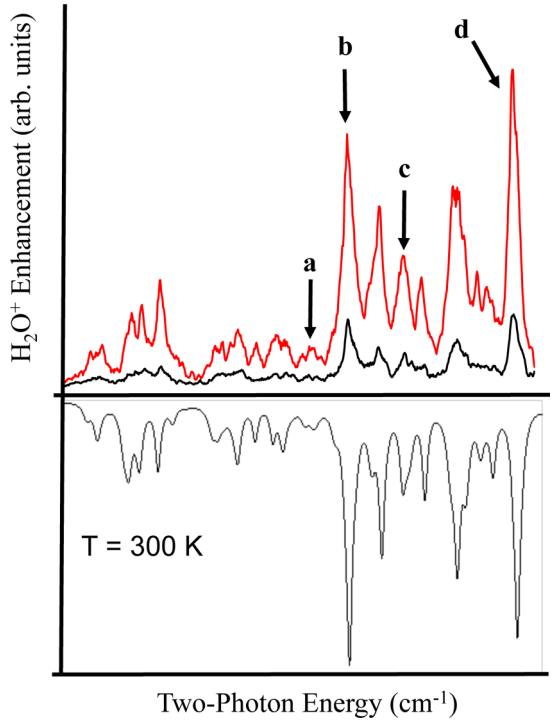

Figure 2. The 2 + 1 REMPI spectra of H_2O via the $\tilde{C}\ ^1B_1(000) \leftarrow \tilde{X}\ ^1A_1(000)$ transition. (Top) The "IR On" spectrum (red) was obtained by exciting the H-bonded OH stretch of $HCl-(H_2O)_3$ at 3550 cm^{-1} and the "IR Off" spectrum (black) by recording the background. The arrows mark the following $J'_{Ka,Kc} \leftarrow J''_{Ka,Kc}$ transtions: (a) $7_{1,7} \leftarrow 7_{1,6}$, (b) $2_{0,2} \leftarrow 3_{2,1}$, (c) $4_{0,4}/4_{1,4} \leftarrow 5_{0,5}/5_{1,5}$, and (d) $2_{0,2} \leftarrow 2_{2,1}$. Assignments are based on the simulated spectrum (300 K) created in PGOPHER (bottom).[30,31]

images were obtained by monitoring H_2O fragments in $J''_{Ka,Kc} = 2_{2,1}$, $3_{2,1}$, and $5_{0,5}/5_{1,5}$.

Figure 3 shows center-of-mass (c.m.) translational energy (E_T) distributions derived from the images. Conservation of energy

DOI: 10.1021/acs.jpclett.6b01848
J. Phys. Chem. Lett. 2016, 7, 4243−4247

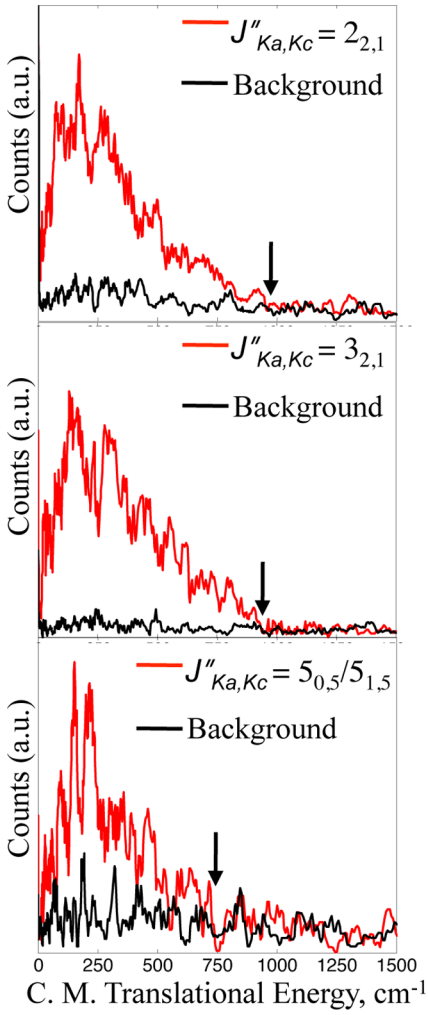

Figure 3. The c.m. translational energy distributions obtained by monitoring state-selected H_2O fragments in $J''_{Ka,Kc}$ levels (a) $2_{2,1}$, (b) $3_{2,1}$, and (c) $5_{0,5}/5_{1,5}$.

can be used to determine the dissociation energy and the pair-correlated rovibrational fragment distributions in the form

$$h\nu_{IR} + E_{int}(HCl{-}(H_2O)_3) = D_0 + E_T + E_{rot}(H_2O) + E_{vib,rot}(HCl{-}(H_2O)_2) \quad (1)$$

Here, $h\nu_{IR}$ is the excitation energy of the H-bonded OH stretch of $HCl{-}(H_2O)_3$, $E_{int}(HCl{-}(H_2O)_3)$ is the cluster's internal energy, $E_{rot}(H_2O)$ is the energy of the monitored $H_2O(J''_{Ka,Kc})$ level, and $E_{vib,rot}(HCl{-}(H_2O)_2)$ is the rovibrational energy of the cofragment. The internal energy of the parent cluster was estimated from the rotational temperature of the H_2O monomers in the molecular beam to be 10 ± 5 cm^{-1}. By monitoring a specific $E_{rot}(H_2O)$ level, the remaining energy (E_{avail}) must be distributed between the internal energy of the cofragment and E_T.

$$E_{avail} = h\nu_{IR} + E_{int}(HCl{-}(H_2O)_3) - D_0 - E_{rot}(H_2O) = E_T + E_{vib,rot}(HCl{-}(H_2O)_2) \quad (2)$$

Note that the energetically allowed internal states of $HCl{-}(H_2O)_2$ are pair-correlated with the individual $H_2O(J''_{Ka,Kc})$ fragment being monitored. As expected, due to the large density of states of $HCl{-}(H_2O)_2$, the E_T distributions are broad, encompassing all of the energetically allowed states, and do not display reproducible structures. At the end point of each image (indicated by the arrows in Figure 3), all of the excess energy is in E_T. This allows the determination of D_0 for Pathway 1.

The maximum values of E_T determined from images of the three $H_2O(J''_{Ka,Kc})$ levels indicated in Figure 3 give D_0 = 2400 ± 100 cm^{-1}. The uncertainty stems mainly from the inaccuracy inherent in using the maximum observed E_T to determine D_0, in the absence of reproducible peaks or features in the E_T distributions.[6] Minor contributions to the error derive from uncertainties in $E_{int}(HCl{-}(H_2O)_3)$ and the calibration of the IR wavelength (see the Supporting Information).

Comparison with previous experimental work on the VP of $HCl{-}H_2O$, $(H_2O)_2$, $(H_2O)_3$, and $(HCl)_3$ can add to our understanding of H-bonding and cooperativity in these mixed clusters.[28,32−34] Assuming that none of the H-bonds in the cyclic tetramer have become weaker than the corresponding bonds in $(H_2O)_2$ and $HCl{-}H_2O$, the weakest bond in the cluster should be O−H···Cl (δ).[35] It is then reasonable that, as in $(H_2O)_3$ and $(HCl)_3$,[4,33,34] after the quantum of the stretch vibration is transferred to the $HCl{-}(H_2O)_3$ ring, VP proceeds by first breaking the O−H···Cl H-bond, forming the chain isomer of the tetramer. In analogy with other cases of small H-bonded dimers and trimers,[4] no barrier is expected in the VP. Subsequently, after further vibrational energy redistribution in the chain isomer, a second bond breaks, releasing H_2O in Pathway 1. The binding energy of the O−H···Cl H-bond in the tetramer has not been determined but is expected to be much smaller than the other H-bonds. [It is probably between the values for the HCl dimer (431 cm^{-1}) and $HCl{-}H_2O$ (1334 cm^{-1}).[4]] Clearly, the sum of this bond energy and that of the $H_2O{-}H_2O$ in the dimer (1105 ± 10 cm^{-1})[34] is smaller than the measured D_0 value for the mixed tetramer, indicating a significant contribution from cooperativity (nonpairwise interactions) to the bonding. In comparison, in the H_2O[33] and HCl[34] trimers, it was shown that ∼19 and ∼22%, respectively, of their D_0 values derive from nonpairwise interactions. Cooperativity is best evaluated by calculations that separate the contributions of two-, three-, and higher multibody interactions to the binding strength. However, it is generally accepted that interactions higher than three-body add only minor contributions to the binding,[4,36,37] and therefore, it is reasonable that for small HCl/H_2O cyclic clusters cooperativity would contribute on the order of 20% to the binding strength. What we do not see so far, however, are any signs of incipient ionization, and the cluster seems to behave in a similar way to the trimers of water and HCl.

In summary, VP of the $HCl{-}(H_2O)_3$ cluster to yield H_2O + $HCl{-}(H_2O)_2$ fragments following excitation of the H-bonded OH stretch fundamental is reported for the first time. This cluster is not expected to lead to acid ionization, and indeed, both neutral H_2O and HCl products have been detected by REMPI following VP. VMI was used to determine D_0 = 2400 ± 100 cm^{-1} for the H_2O + $HCl{-}(H_2O)_2$ pathway. The rotational energy distributions in the H_2O and $HCl{-}(H_2O)_2$ fragments are broad and encompass all of the internal states allowed by energy conservation. Cooperativy contributions appear to be significant and of the same order of magnitude as those reported before in theoretical and experimental studies of the water and HCl trimers. Experiments to observe Pathway 2 are currently underway in our lab. Hopefully, the present results will lead to more theoretical work on the vibrational assignments and VP mechanisms of these mixed clusters.

DOI: 10.1021/acs.jpclett.6b01848
J. Phys. Chem. Lett. 2016, 7, 4243−4247

METHODS

The experimental procedures are similar to those employed in previous work on smaller H-bonded clusters.[6] The mixed HCl/H_2O clusters were formed in supersonic expansion through a 0.5 mm orifice of a pulsed valve (~150 μs opening time). The sample concentration and backing pressure were optimized for maximum signal of the HCl−$(H_2O)_3$ tetramer at 0.6% H_2O and 2% HCl (99.995%) in ~2 atm of helium (99.999%). At these concentrations, signals from pure water clusters and from clusters with higher HCl/H_2O ratios were minimized (see the Supporting Information for details). The mixture was introduced into a high-vacuum chamber maintained at a base pressure of $\sim 3.0 \times 10^{-8}$ Torr.

The skimmed molecular beam was intersected at right angles by two anticollinear laser beams. Focused IR laser radiation (OPO/OPA system, ~3.5 mJ/pulse; 20 cm lens, 0.4 cm^{-1} bandwidth) was used to excite the OH stretch of the cluster, and focused UV radiation (0.1−0.4 mJ/pulse; 20 cm lens) was used to probe H_2O fragments. The IR frequency was calibrated using ammonia in a photoacoustic cell. The UV radiation was calibrated using a simulated REMPI spectrum of H_2O.[30,31]

Two modes of detection were used to collect data: (i) TOF-MS for spectroscopic investigations and (ii) VMI for E_T distributions. In "IR On" signal was collected when firing the IR laser ~70 ns before the UV laser, whereas in "IR Off", it was fired ~2 μs after the UV laser. The laser conditions (timing, focusing, power) were optimized to enhance the signal from HCl−$(H_2O)_3$ while minimizing signals from other clusters.

The VMI arrangement has been described previously.[6] It consists of a four-electrode ion acceleration assembly, a 60 cm field-free drift tube, and a microchannel (MCP) detector coupled to a phosphor screen that is monitored by a CCD camera. The two-dimensional projections were reconstructed using the BASEX method. The velocity (m/s) of the detected H_2O^+ fragments was proportional to 3.67 times the number of pixels on our detector.

Reducing the UV power eliminated signals from multiphoton UV processes, and background H_2O monomer signals were minimized by cryopumping with a coldfinger liquid nitrogen trap. Minimizing the IR-dependent background from higher clusters was crucial for our VMI results. Background images at 3651.8 cm^{-1} (the nearest energetically cluster-free region) were taken before and after each image. Typically, signal and background images were recorded intermittently for 10−12 h at 10 Hz.

ASSOCIATED CONTENT

Supporting Information

The Supporting Information is available free of charge on the ACS Publications website at DOI: 10.1021/acs.jpclett.6b01848.

Assignments for the H-bonded OH stretch fundamentals for $(HCl)_m$−$(H_2O)_n$, $m = 0$−3 and $n = 1$−3, in the region of 3525−3640 cm^{-1} and discussion of errors (PDF)

AUTHOR INFORMATION

Corresponding Author

*E-mail: reisler@usc.edu.

Notes

The authors declare no competing financial interest.

ACKNOWLEDGMENTS

The authors thank Professor Joel Bowman, Dr. John Mancini, and Professor Andrey Vilesov for many enlightening discussions and for communicating results prior to publication. This work is supported by the National Science Foundation Grant No. CHE-1265725.

REFERENCES

(1) Anderson, J. G.; Toohey, D. W.; Brune, W. H. Free Radicals Within the Antarctic Vortex: The Role of CFCs in Antarctic Ozone Loss. *Science* **1991**, *251*, 39−46.

(2) Solomon, S. Progress Towards a Quantitative Understanding of Antarctic Ozone Depletion. *Nature* **1990**, *347*, 347−354.

(3) Gerber, R. B.; Varner, M. E.; Hammerich, A. D.; Riikonen, S.; Murdachaew, G.; Shemesh, D.; Finlayson-Pitts, B. J. Computational Studies of Atmospherically-Relevant Chemical Reactions in Water Clusters and on Liquid Water and Ice Surfaces. *Acc. Chem. Res.* **2015**, *48*, 399−406.

(4) Samanta, A. K.; Wang, Y.; Mancini, J. S.; Bowman, J. M.; Reisler, H. Energetics and Predissociation Dynamics of Small Water, HCl, and Mixed HCl−Water Clusters. *Chem. Rev.* **2016**, *116*, 4913−4936.

(5) Samanta, A. K.; Czakó, G.; Wang, Y.; Mancini, J. S.; Bowman, J. M.; Reisler, H. Experimental and Theoretical Investigations of Energy Transfer and Hydrogen-Bond Breaking in Small Water and HCl Clusters. *Acc. Chem. Res.* **2014**, *47*, 2700−2709.

(6) Samanta, A. K.; Ch'ng, L. C.; Reisler, H. Imaging Bond Breaking and Vibrational Energy Transfer in Small Water Containing Clusters. *Chem. Phys. Lett.* **2013**, *575*, 1−11.

(7) Bacelo, D. E.; Binning, R. C., Jr.; Ishikawa, Y. *Ab Initio* Monte Carlo Simulated Annealing Study of $HCl(H_2O)_n$ (n = 3, 4) Clusters. *J. Phys. Chem. A* **1999**, *103*, 4631−4640.

(8) Re, S.; Osamura, Y.; Suzuki, Y.; Schaefer, H. F. Structures and Stability of Hydrated Clusters of Hydrogen Chloride, $HCl(H_2O)_n$, n = 1−5. *J. Chem. Phys.* **1998**, *109*, 973−977.

(9) Packer, M. J.; Clary, D. C. Interaction of HCl with Water Clusters: $(H_2O)_nHCl$, n = 1−3. *J. Phys. Chem.* **1995**, *99*, 14323−14333.

(10) Chaban, G. M.; Gerber, R. B.; Janda, K. C. Transition from Hydrogen Bonding to Ionization in $(HCl)_n(NH_3)_n$ and $(HCl)_n(H_2O)_n$ Clusters: Consequences for Anharmonic Vibrational Spectroscopy. *J. Phys. Chem. A* **2001**, *105*, 8323−8332.

(11) Andot, K.; Hynes, J. T. HCl Acid Ionization in Water: A Theoretical Molecular Modeling. *J. Mol. Liq.* **1995**, *64*, 25−37.

(12) Masia, M.; Forbert, H.; Marx, D. Connecting Structure to Infrared Spectra of Molecular and Autodissociated HCl−Water Aggregates. *J. Phys. Chem. A* **2007**, *111*, 12181−12191.

(13) Sugawara, S.; Yoshikawa, T.; Takayanagi, T.; Tachikawa, M. Theoretical Study on Mechanisms of Structural Rearrangement and Ionic Dissociation in the $HCl(H_2O)_4$ Cluster with Path-Integral Molecular Dynamics Simulations. *Chem. Phys. Lett.* **2011**, *501*, 238−244.

(14) Forbert, H.; Masia, M.; Kaczmarek-Kedziera, A.; Nair, N. N.; Marx, D. Aggregation-Induced Chemical Reactions: Acid Dissociation in Growing Water Clusters. *J. Am. Chem. Soc.* **2011**, *133*, 4062−4072.

(15) Mancini, J. S.; Bowman, J. M. Isolating the Spectral Signature of H_3O^+ in the Smallest Droplet of Dissociated HCl Acid. *Phys. Chem. Chem. Phys.* **2015**, *17*, 6222−6226.

(16) Vargas-Caamal, A.; Cabellos, J. L.; Ortiz-Chi, F.; Rzepa, H. S.; Restrepo, A.; Merino, G. How Many Water Molecules Does It Take to Dissociate HCl? *Chem. - Eur. J.* **2016**, *22*, 2812−2818.

(17) Hassanali, A. A.; Cuny, J.; Ceriotti, M.; Pickard, C. J.; Parrinello, M. The Fuzzy Quantum Proton in the Hydrogen Chloride Hydrates. *J. Am. Chem. Soc.* **2012**, *134*, 8557−8569.

(18) Walewski, Ł.; Forbert, H.; Marx, D. Revealing the Subtle Interplay of Thermal and Quantum Fluctuation Effects on Contact Ion Pairing in Microsolvated HCl. *ChemPhysChem* **2013**, *14*, 817−826.

(19) Fárník, M.; Weimann, M.; Suhm, M. A. Acidic Protons before Take-Off: A Comparative Jet Fourier Transform Infrared Study of Small

DOI: 10.1021/acs.jpclett.6b01848
J. Phys. Chem. Lett. 2016, 7, 4243−4247

HCl− and HBr−Solvent Complexes. *J. Chem. Phys.* **2003**, *118*, 10120−10136.
(20) Zischang, J.; Skvortsov, D.; Choi, M. Y.; Mata, R. A.; Suhm, M. A.; Vilesov, A. F. Helium Nanodroplet Study of the Hydrogen-Bonded OH Vibrations in HCl−H_2O Clusters. *J. Phys. Chem. A* **2015**, *119*, 2636−2643.
(21) Letzner, M.; Gruen, S.; Habig, D.; Hanke, K.; Endres, T.; Nieto, P.; Schwaab, G.; Walewski, Ł.; Wollenhaupt, M.; Forbert, H.; Marx, D.; Havenith, M. High Resolution Spectroscopy of HCl−water Clusters: IR Bands of Undissociated and Dissociated Clusters Revisited. *J. Chem. Phys.* **2013**, *139*, 154304.
(22) Skvortsov, D.; Lee, S. J.; Choi, M. Y.; Vilesov, A. F. Hydrated HCl Clusters, $HCl(H_2O)_{1-3}$ in Helium Nanodroplets: Studies of Free OH Vibrational Stretching Modes. *J. Phys. Chem. A* **2009**, *113*, 7360−7365.
(23) Flynn, S. D.; Skvortsov, D.; Morrison, A. M.; Liang, T.; Choi, M. Y.; Douberly, G. E.; Vilesov, A. F. Infrared Spectra of HCl−H_2O Clusters in Helium Nanodroplets. *J. Phys. Chem. Lett.* **2010**, *1*, 2233−2238.
(24) Morrison, A. M.; Flynn, S. D.; Liang, T.; Douberly, G. E. Infrared Spectroscopy of $(HCl)_m(H_2O)_n$ Clusters in Helium Nanodroplets: Definitive Assignments in the HCl Stretch Region. *J. Phys. Chem. A* **2010**, *114*, 8090−8098.
(25) Amirand, C.; Maillard, D. Spectrum and Structure of Water-Rich Water—Hydracid Complexes from Matrix Isolation Spectroscopy: Evidence for Proton Transfer. *J. Mol. Struct.* **1988**, *176*, 181−201.
(26) Mancini, J. S.; Bowman, J. M. Effects of Zero-Point Delocalization on the Vibrational Frequencies of Mixed HCl and Water Clusters. *J. Phys. Chem. Lett.* **2014**, *5*, 2247−2253.
(27) Odde, S.; Mhin, B. J.; Lee, S.; Lee, H. M.; Kim, K. S. Dissociation Chemistry of Hydrogen Halides in Water. *J. Chem. Phys.* **2004**, *120*, 9524−9535.
(28) Rocher-Casterline, B. E.; Mollner, A. K.; Ch'ng, L. C.; Reisler, H. Imaging H_2O Photofragments in the Predissociation of the HCl−H_2O Hydrogen-Bonded Dimer. *J. Phys. Chem. A* **2011**, *115*, 6903−6909.
(29) Guggemos, N.; Slavíček, P.; Kresin, V. V. Electric Dipole Moments of Nanosolvated Acid Molecules in Water Clusters. *Phys. Rev. Lett.* **2015**, *114*, 043401.
(30) Western, C. M. *PGOPHER*, a Program for Simulating Rotational, Vibrational, & Electronic Spectra; University of Bristol: Bristol, U.K., 2016; http://pgopher.chm.bris.ac.uk.
(31) Yang, C.-H.; Sarma, G.; ter Meulen, J. J.; Parker, D. H.; Western, C. M. REMPI Spectroscopy and Predissociation of the $C^1B_1(v= 0)$ Rotational Levels of H_2O, HOD and D_2O. *Phys. Chem. Chem. Phys.* **2010**, *12*, 13983−13991.
(32) Rocher-Casterline, B. E.; Ch'ng, L. C.; Mollner, A. K.; Reisler, H. Communication: Determination of the Bond Dissociation Energy (D_0) of the Water Dimer, $(H_2O)_2$, by Velocity Map Imaging. *J. Chem. Phys.* **2011**, *134*, 211101.
(33) Ch'ng, L. C.; Samanta, A. K.; Wang, Y.; Bowman, J. M.; Reisler, H. Experimental and Theoretical Investigations of the Dissociation Energy (D_0) and Dynamics of the Water Trimer, $(H_2O)_3$. *J. Phys. Chem. A* **2013**, *117*, 7207−7216.
(34) Mancini, J. S.; Samanta, A. K.; Bowman, J. M.; Reisler, H. Experiment and Theory Elucidate the Multichannel Predissociation Dynamics of the HCl Trimer: Breaking Up is Hard to Do. *J. Phys. Chem. A* **2014**, *118*, 8402−8410.
(35) Kisiel, Z.; Białkowska-Jaworska, E.; Pszczółkowski, L.; Milet, A.; Struniewicz, C.; Moszynski, R.; Sadlej, J. Structure and Properties of the Weakly Bound Trimer $(H_2O)_2$...HCl Observed by Rotational Spectroscopy. *J. Chem. Phys.* **2000**, *112*, 5767−5776.
(36) Xantheas, S. S. Ab initio Studies of Cyclic Water Clusters $(H_2O)_n$, n = 1−6. II. Analysis of Many-Body Interactions. *J. Chem. Phys.* **1994**, *100*, 7523−7534.
(37) Mancini, J. S. *Computational Studies on the Anharmonic Dynamics of Molecular Clusters*. Ph.D. Dissertation [Online], Emory University, Atlanta, GA, 2015; http://pid.emory.edu/ark:/25593/mr710.

DOI: 10.1021/acs.jpclett.6b01848
J. Phys. Chem. Lett. 2016, 7, 4243−4247